




# Improving Steel and Steelmaking—an Ionic Liquid Database for Alloy Process Design

David Dilner<sup>1,2</sup> · Lina Kjellqvist<sup>3</sup> · Huahai Mao<sup>1,3</sup> · Malin Selleby<sup>1</sup> 

Received: 31 August 2018 / Accepted: 21 November 2018 / Published online: 7 December 2018  
© The Author(s) 2018

## Abstract

The latest development of a thermodynamic database is demonstrated with application examples related to the steelmaking process and steel property predictions. The database, TCOX, has comprehensive descriptions of the solution phases using ionic models. More specifically, applications involving sulphur and oxygen, separately as well as combined, are presented and compared with relevant multi-component experimental information found in the literature. The over-all agreement is good.

**Keywords** CALPHAD · Ionic 2-sublattice liquid model · Steelmaking · Inclusions · Sulphide · Oxide

## Introduction

Customer demand on higher performance and increased competition on the global steel market make it even more desirable to produce better steels at a lower cost. An important factor to consider when developing new steels is the presence of inclusions [1]. Their amount, type and size are of importance for the properties of the final product. Another important factor to consider is the steel's corrosion resistance, as corrosion is very costly as it dramatically shortens the lifetime of steel products. Almost all iron ore is iron oxide minerals and among them hematite is the most common. During primary steelmaking, oxygen is used to lower the carbon content of the crude iron. In secondary steelmaking [2], slags which mostly consist of

oxides are used to protect the steel and to absorb impurities. Oxide inclusions can have a detrimental impact on the mechanical properties of steel. Finally, oxygen is the main element responsible for corrosion of steels, when nature wants to reclaim the steel, rust, i.e. iron oxide, is formed. In addition to oxygen, sulphur is an important element for steelmaking and steel properties [3]. Even though red-shortness, melting of iron sulphide at forging temperatures, rarely or never occurs today, sulphides are an important type of inclusion which often have a negative impact on mechanical properties. Manganese was early on used to tackle the problem of red-shortness and it is, for many reasons, a common alloying element today. Additionally, calcium is now commonly used as a sulphide former. Both MnS and CaS influence the mechanical properties of steel, particularly the impact toughness. Due to relatively high melting points of sulphides with chromium or nickel, red-shortness is not a problem in stainless steels. In addition, stainless steels are usually alloyed with other sulphide-forming elements, like calcium, manganese or titanium. The sulphides in stainless steels do not only impact the mechanical properties but also the corrosion resistance. More specifically, sulphides play a major role in pitting corrosion [4] which may be detrimental in high temperature applications.

It is essential to understand and describe the thermodynamic properties to be able to predict the influence of oxygen and sulphur during the steelmaking process and on the final steel properties. An efficient way to make equilibrium calculations is to use the CALPHAD-method [5]. In particular, the compound energy formalism (CEF) [6–8] has proven useful for modelling solutions phases. The model for liquid phases

---

✉ Malin Selleby  
malin@kth.se

David Dilner  
research@dilner.se

Lina Kjellqvist  
lina@thermocalc.se

Huahai Mao  
huahai@kth.se

<sup>1</sup> Materials Science and Engineering, KTH Royal Institute of Technology, Brinellvägen 23, SE-100 44 Stockholm, Sweden

<sup>2</sup> Present address: Scania CV AB, SE-151 87 Södertälje, Sweden

<sup>3</sup> Thermo-Calc Software AB, Råsundavägen 18, SE-169 67 Solna, Sweden

within the formalism is the ionic two-sublattice liquid model that has been revised over the years since its introduction [9, 10]. This model is used in the TCOX database [11] in the Thermo-Calc package which contains a thermodynamic description involving many oxide systems. The COMPASS project, supported by the Swedish industry, had the ambition to improve the description in TCOX, mainly by adding sulphur to the database. In this paper, the present state of the TCOX database is demonstrated with calculations involving oxygen and sulphur, separately as well as combined. It should be emphasized that all calculations are done with TCOX alone as the ionic two-sublattice model is able to describe both the metallic liquid and the liquid slag—they merely have different compositions, i.e. are separated by a miscibility gap.

The latest update of the TCOX database includes the addition of 12 new elements: Ar, Co, Cu, F, Gd, La, Mo, Nb, P, S, V and W. Thus, the database now contains thermodynamic data for the following 24 elements: Al, Ar, C, Ca, Co, Cr, Cu, F, Fe, Gd, La, Mg, Mn, Mo, Nb, Ni, O, P, S, Si, V, W, Y and Zr. The intended application is for solid and liquid ionized materials, i.e. oxides, sulphides, fluorides and silicates, or a mixture of these. Applications could include development of ceramics, slags, refractories, metallurgical processing, ESR slags, material corrosion, thermal barrier coatings (TBC), yttria-stabilized-zirconia (YSZ), solid oxide fuel cell materials, sulphide formation and desulphurization, to name a few uses of the database. The scope of this paper will however limit itself to applications related to steels and steelmaking. Calculations related to steel and steelmaking are made and compared with experimental findings in studies found in various published papers. A large number of papers were found, however, only a few were found suitable to compare with calculations as the majority did not present data in a way that could be reproduced, e.g. too little information was provided or uncertainties regarding the boundary conditions were found.

## Calculations Involving Oxygen

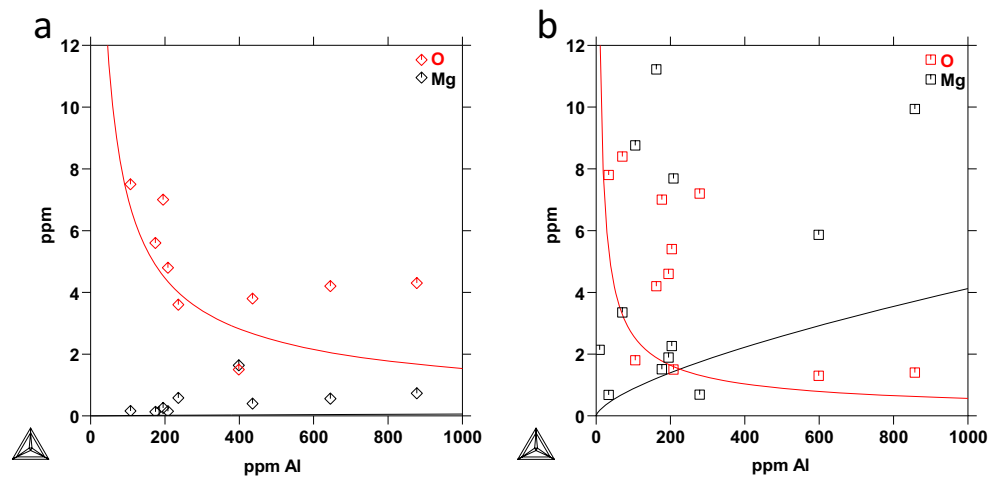
As mentioned in the ‘Introduction’, the TCOX database contains a thermodynamic description involving many oxide systems. The major alloying elements in steels, Fe, C, Cr, Ni and Mn, and the major slag components,  $\text{Al}_2\text{O}_3$ , CaO, MgO and  $\text{SiO}_2$ , are included. In addition, some other important oxide-forming elements have been included in the database. In this part of the paper, three application examples related to oxygen during steelmaking are presented.

Aluminium is commonly used in deoxidation of steels and thus understanding this process is of importance to optimize steelmaking. During this process, the spinel phase ( $\text{MgO}\cdot\text{Al}_2\text{O}_3$ ) is often observed, which motivated Seo et al. [12] to equilibrate iron with additions of small amounts of aluminium and magnesium together with spinel ( $\text{MgO}\cdot\text{Al}_2\text{O}_3$ ), in either

alumina or magnesia crucibles. The equilibration was performed at 1600 °C for 30 min. In Fig. 1, their results are compared with the calculated results from TCOX [11] for which it was assumed that the liquid steel was in equilibrium with the spinel and  $\text{Al}_2\text{O}_3$  or MgO respectively. As can be seen, a reasonable agreement is obtained but the experimental results show a rather large scatter.

In stainless steels, the addition of alloying elements is the major cost. Nickel is the most expensive element both due to its price and the considerable amounts used in many stainless steel grades. However, nickel is less reactive than iron and thus tends to stay in the steel. This means that any major cost reduction involving nickel requires the nickel content in the final steel to be lowered, i.e. a new steel grade has to be developed. Chromium, on the other hand, is more reactive than iron and tends to end up in the slag. Even though chromium is far from as expensive as nickel, the large amount of chromium used in stainless steels means that it still presents a large cost. Thus, optimizing the steelmaking process to minimize chromium loss would be beneficial. Another alternative is to retrieve chromium from the slag afterwards. This has been investigated by Nakasuga et al. [13] and in their study, they investigate the recovery rate of chromium for different  $\text{SiO}_2$  contents. They equilibrated 120 g steel synthetic crude iron (i.e. pure Fe-C) with 10 g slag, adding 0.6, 1.2 and 2.4 g  $\text{SiO}_2$ . The initial slag composition was reported to be 2.66 mass%  $\text{Cr}_2\text{O}_3$ , 5.2 mass% FeO, 44.57 mass% CaO, 33.06 mass%  $\text{SiO}_2$ , 3.59 mass%  $\text{Al}_2\text{O}_3$ , 8.33 mass% MgO, 0.44 mass% MnO and 2.15 mass%  $\text{TiO}_2$ . Their reported final recovery at 1400 °C is presented in Fig. 2 together with calculated results. In the calculations, the synthetic crude iron is assumed to be pure iron, i.e. neglecting the carbon content, and the calculation included the same system as used by Nakasuga et al. The chromium recovery is defined as  $R_{\text{Cr}} = n_{\text{Cr,steel}}/n_{\text{Cr,tot}}$ . In addition, the reported slag liquidus temperature is presented with the present calculated results in Fig. 3. The calculated liquidus temperature is estimated as the temperature where only liquid and spinel are present, since a small amount of spinel is present over a large temperature interval this would probably be difficult to detect experimentally. Since titanium is not yet included in the TCOX database, this element was neglected in the calculations which could slightly affect the result. In general, the agreement with their experimental results concerning chromium is good. The sudden decrease in chromium recovery at high  $\text{SiO}_2$  content, observed experimentally, could be explained by the fact that reaction kinetics become slower at higher  $\text{SiO}_2$  contents due to higher viscosity. The change in slope is related to different phases being present, at lower  $\text{SiO}_2$  content spinel is present while at the higher  $\text{SiO}_2$  content it melts. A possible explanation of why this is not mentioned in the experimental paper is that the authors were focusing on reaction rate rather than the equilibrium state. It is also reasonable that the calculated chromium recovery should be higher than the experimentally reported.

**Fig. 1** The calculated and experimental oxygen (red) and magnesium (black) content in liquid steel at 1600 °C in equilibrium with  $\text{MgAl}_2\text{O}_4$ -spinel using **a**  $\text{Al}_2\text{O}_3$  crucible and **b**  $\text{MgO}$  crucible with data from Seo et al. [12]



The understanding of oxide scale formation on alloyed steels is important to be able to estimate the corrosion resistance as different oxides have fundamentally different behavior in corrosive environments. Compare for instance rust with the protective chromium oxide layers of stainless steels. The oxidation of an austenitic stainless steel has been studied by Douglass et al. [14]. The samples were oxidized over the temperature range 700–1000 °C for 24 h. However, it seemed like equilibrium was not reached for the samples at low temperatures, where the only oxide formed in their experiments after 24 h was  $\text{Mn}_2\text{O}_3$ , while at higher temperatures, the oxide scales formed were thick and complex. At high temperatures, the outermost oxide was always  $\text{Mn}_2\text{O}_3$  with some dissolved iron. In some cases, a thin layer of  $\text{Fe}_2\text{O}_3$  with dissolved manganese was found beneath the  $\text{Mn}_2\text{O}_3$  layer. Below the outer scale, an Fe-Mn rich spinel was formed and closest to the substrate a layer with manganowustite and a Cr-rich spinel. A thermodynamic equilibrium calculation on the oxidation of a steel at 900 °C is shown in Fig. 4a and the composition of the spinel phase is shown in Fig. 4b. At highest  $P_{\text{O}_2}$ ,

some  $\text{Mn}_2\text{O}_3$  is stable. The corundum phase has a composition close to  $\text{Fe}_2\text{O}_3$ , with some Cr and Mn dissolved. As seen in Fig. 4b, the spinel phase has a composition very close to  $\text{MnCr}_2\text{O}_4$  at low  $P_{\text{O}_2}$ , with an increasing amount of Fe at higher  $P_{\text{O}_2}$ . The composition of the halite phase is close to MnO at low  $P_{\text{O}_2}$  and a more Fe-rich phase at high  $P_{\text{O}_2}$ . Overall, the calculated result is in good agreement with the experimental findings, although it is difficult to show in the calculated diagrams. Though, it should be remembered that this is a simple equilibrium calculation (no diffusion is taken into account) and it is not possible to get the thickness of the different layers. To be able to do such a calculation, mobility data for the different oxides need to be assessed and a diffusion simulation software, like DICTRA, has to be used.

## Calculations Involving Sulphur

As mentioned in the ‘Introduction’, one of the major aims with this paper is to demonstrate how the new sulphide description

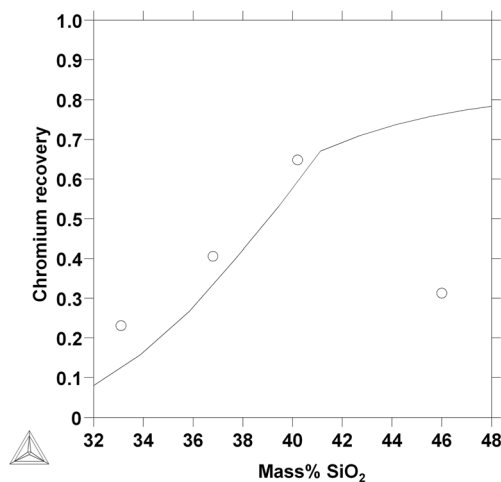


**Fig. 2** Calculated chromium recovery ( $R_{\text{Cr}} = n_{\text{Cr,steel}}/n_{\text{Cr,tot}}$ ) as a function of  $\text{SiO}_2$  content at 1400 °C together with experimental data from Nakasuga et al. [13]

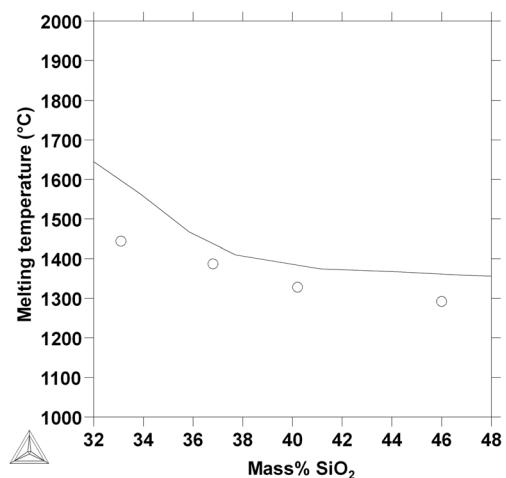
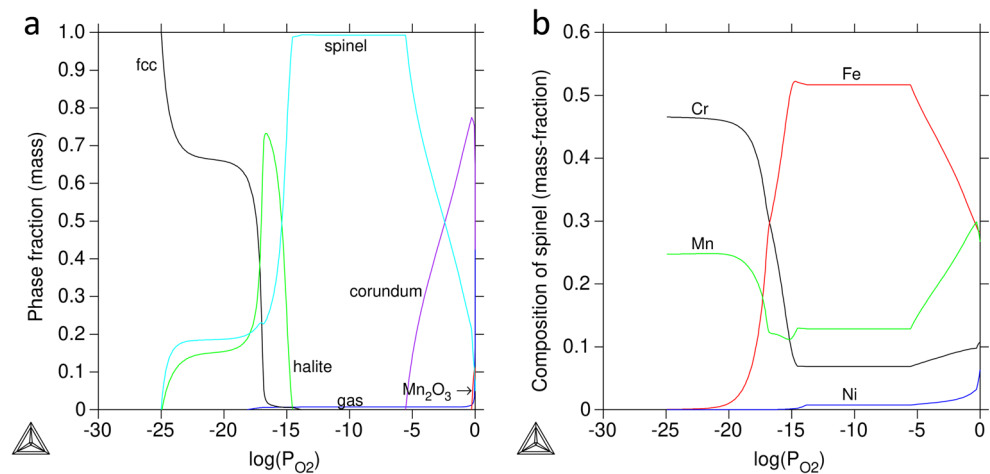


**Fig. 3** Calculated slag melting (liquidus) temperature as a function of  $\text{SiO}_2$  together with experimental data Nakasuga et al. [13]

**Fig. 4** Oxidation of a steel (17.8 mass% Mn, 9.5 mass% Cr, 1.0 mass% Ni, 0.27 mass% C) at 900 °C. **a** Stable phases and **b** composition of the spinel phase



in TCOX can be used to make reliable calculations related to sulphur in steels. The ambition has been to compare calculations with experimental results. However, it must be mentioned that the number of suitable publications for this purpose is limited. Some binary or ternary systems have been investigated, but they were already used in the assessments of the subsystems and therefore cannot be used to validate the database. Other investigations are concerned with systems consisting of several elements not included in this description. In addition, reports on larger systems are usually concerned with process data and thus not equilibrium. Despite this, some useful results have been found in the literature.

Large efforts have been made to describe the thermodynamics of the Fe-Mn-Ca-Mg-S system, as presented in previous works [15–18]. Other low order systems are also needed in order to be able to make calculations related to steels and steelmaking, in particular stainless steels where chromium and nickel are the dominating alloying elements. In a parallel work [19], the system Fe-Cr-Cu-Ni-S is assessed using compatible models for all phases.

MnS is the most common sulphide in low alloyed steels and due to this, it is important to be able to predict its formation. For this reason, several thermodynamic assessments have been concerned with the Fe-Mn-S system both earlier [20–23], and as part of this work [15]. Another sulphide which is common in many low alloyed steels is CaS which motivated thermodynamic assessments including calcium and sulphur [17, 18]. An important property in predicting the formation of sulphides is the formation temperature. The formation temperature of MnS has been reported by Wriedt and Hu [24]. They used a 3%-Si steel with and without calcium additions. In Fig. 5, the calculated mass fraction MnS is plotted as a function of temperature. The steel compositions used in the experiment and the calculations are given in the figures. In addition, the highest temperature where MnS is observed and the lowest temperature without MnS from the experimental study are shown as comparison. The agreement with the

experimental results is very good in both cases. It should be mentioned that the lower dissolution temperature of MnS observed in the Ca-containing steel is caused by the fact that the sulphur is bound as CaS rather than MnS.

In stainless steels, it is also possible to find MnS. However, MnS has a high solubility of CrS and due to the large content of chromium in steels these sulphides usually contain a considerable amount of chromium. Since chromium is the fundamental alloying element in stainless steel, this could be of importance. It has even been suggested that chromium depletion around sulphides, due to their chromium uptake, causes pitting corrosion [25]. Given the demanding applications where stainless steels are used, like power plants, increasing the lifetime or service temperature, under which the steel may be used, can be a great competitive advantage. The chromium content dissolved in MnS has been investigated by Henthorne [26]. However, it is not specified at which temperature these results are obtained but it is assumed that it is during casting. The experimental results are compared with the calculated results at two temperatures in Fig. 6. The trend is similar, although the composition deviates which is likely due to the fact that the casting process is too fast for equilibrium to be reached.

Ono and Kohno [27] studied the effect on inclusion composition on the stability of inclusions of 18–8 stainless steel. The composition of the sulphides has been changed by varying the Mn concentration of the steels. The specimens have the following composition: C (0.06–0.07 mass%), Si (0.6–0.71 mass%), S (0.108–0.221 mass%), Ni (8.36–8.55 mass%), Cr (18.20–18.26 mass%), Mn (0.07–1.65 mass%). The calculated composition of the sulphides is shown in Fig. 7. At low Mn concentration, CrS (pyrrhotite) is the stable sulphide and at high Mn concentration, the stable sulphide is MnS (alabandite). Between 0.4–0.5% Mn, there is a mixture of the two different sulphides. The agreement with the experimental data is very good; except for that the calculations show lower solubility of Fe in MnS than the experiments indicate.

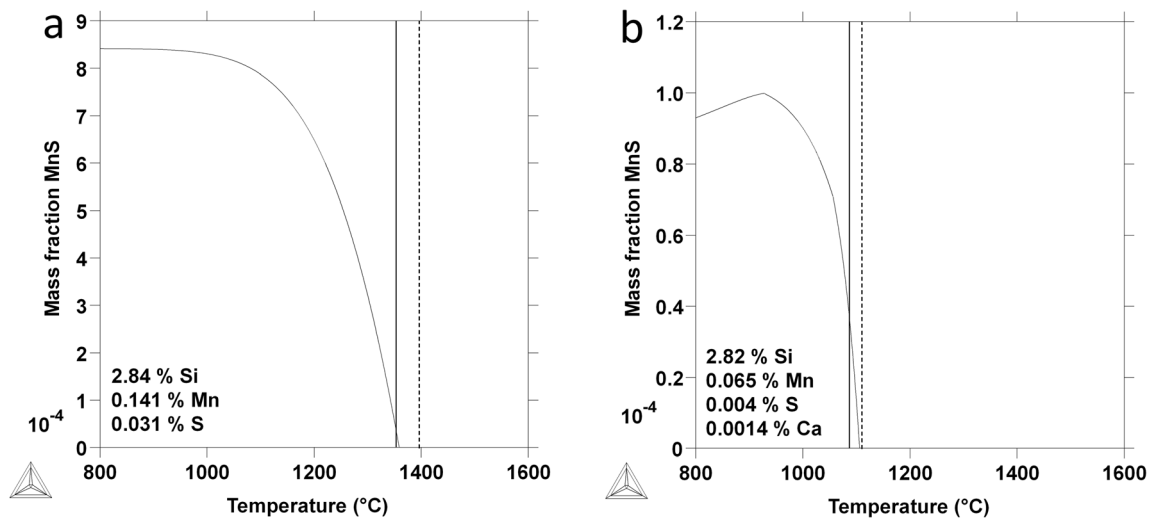


**Fig. 5** Calculated mass fraction MnS with the highest temperature where MnS is observed experimentally as a solid horizontal line and the lowest temperature without MnS observation as a dotted horizontal line for **a**

Mn-alloyed Si-steel and **b** a Si-steel alloyed with both Mn and Ca with data from Wriedt and Hu [24]

### Combining Oxygen and Sulfur

The final part of this paper discusses the combination of the existing TCOX database and the recently developed sulphur descriptions. The key system for such a combination is the Fe-Ca-O-S system which is presented in a separate work [28]. As mentioned in that paper, the ionic two-sublattice liquid model seems to give very good extrapolations between oxide and sulphide systems. Moreover, the solubility of sulphur in solid oxide phases and oxygen in solid sulphide phases seem to be very low.

Since slags are an essential part of steelmaking it is important to be able to predict how the sulphur is distributed between steel and slag. In an effort to demonstrate how genetic alloy design can be used to optimize the steelmaking process, it was found that the equilibrium sulphur content had a major impact on the result [29]. The equilibrium sulfur content

depends to a large extent on the slag composition. Commonly, the concept of sulphide capacity is used as a measure on how effective a certain slag is in absorbing sulphur. However, using computational thermodynamics, this concept becomes obsolete as the sulphur content of the steel can be readily obtained directly from the calculation. O'Neill and Mavrogenes [30] investigated the equilibrium sulphur content in different slags with high SiO<sub>2</sub> contents. They presented data for different sulphur and oxygen partial pressures. In Fig. 8, their results are compared with the present calculated results at  $\log(\text{PO}_2) = -10.28$ . The results show a similar trend although with a difference in sulphur content of the slag.

In addition to oxide components in the slag, it is common to add CaF<sub>2</sub> as a flux agent. Since CaF<sub>2</sub> will take part in thermochemical reactions occurring during steelmaking, it is

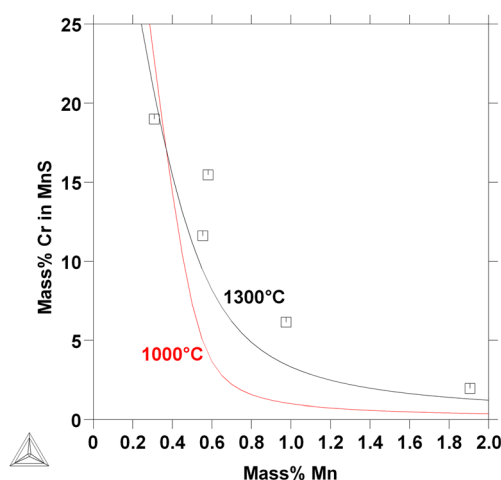


**Fig. 6** Calculated mass% Cr in MnS at two different temperature as lines and experimentally reported results, from Henthorne [26], as squares

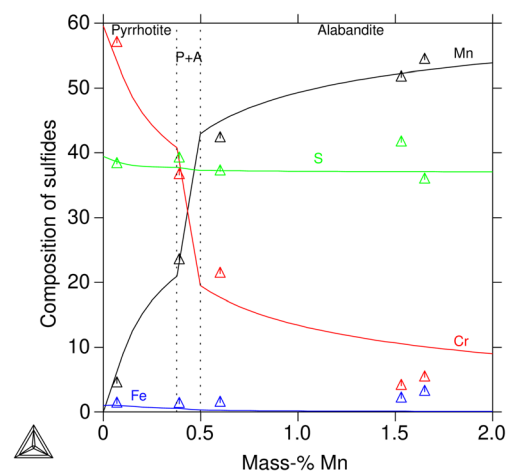


**Fig. 7** The composition of stable sulphides at 1100 °C, in the steels with varying Mn content while the rest of alloying elements fixed 0.06 mass% C, 0.6 mass% Si, 0.2 mass% S, 8.4 mass% Ni and 18.2 mass% Cr with experimental data from Ono and Kohno [27]

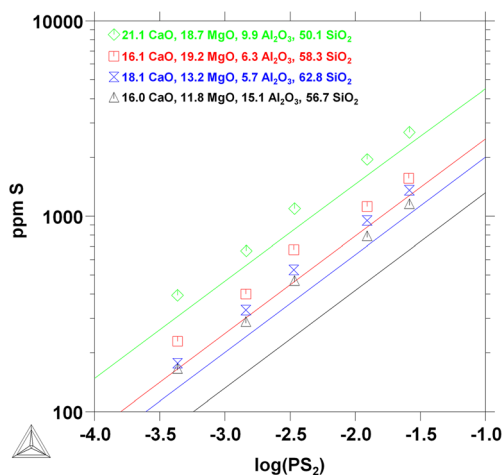


**Fig. 8** Calculated and experimental sulphur content at different sulphur partial pressure for four different slags at 1400 °C, obtained at  $\log(\text{PO}_2) = -10.28$  with data from O'Neill and Mavrogenes [30]

important to predict its effect on the sulphur solubility. This was investigated by Ban-ya et al. [31] on CaO-Al<sub>2</sub>O<sub>3</sub>-CaF<sub>2</sub> slags. In their study, they present sulphur solubility at different CaF<sub>2</sub>:Al<sub>2</sub>O<sub>3</sub> ratios. Their results are shown together with calculated results in Fig. 9. As can be seen, the agreement is very good.

Sulphur capacity is a measure of the slag's ability to dissolve sulphur from the steel. As this is a very important part of steelmaking, in particular when producing speciality steels, many sulphide capacity measurements have been performed for a variety of slag systems over the years, but the results are very scattered. In most measurements, the sulphur pressure in the gas has been determined by using a mixture of SO<sub>2</sub> and

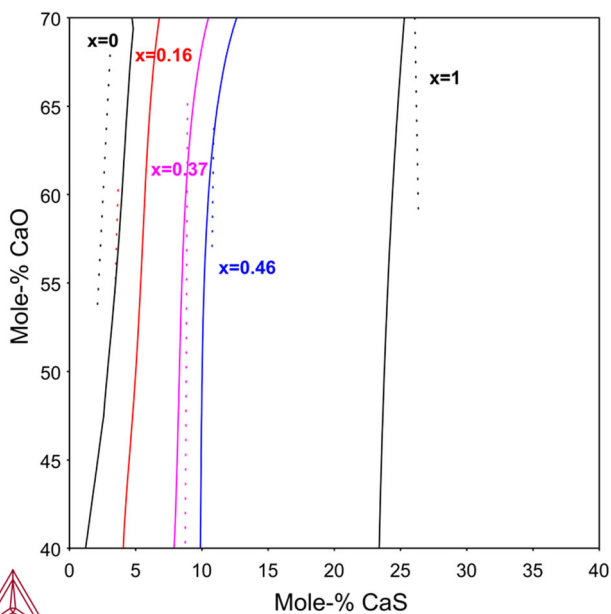


**Fig. 9** Calculated (solid lines) and experimental (dotted lines) sulphur solubility in the CaO-(1-x)Al<sub>2</sub>O<sub>3</sub>-xCaF<sub>2</sub> system at 1600 °C and different Al<sub>2</sub>O<sub>3</sub>:CaF<sub>2</sub> ratios with data from Ban-ya et al. [31]

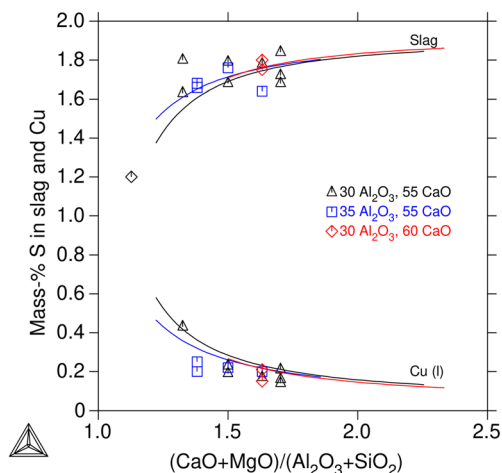


**Fig. 10** Calculated and experimental sulphur content in liquid copper and slag at 1600 °C with data from Allertz and Sichen [32]

other species, but it is difficult to control the gas using this technique. Allertz and Sichen [32] used a different method by using a copper-slag equilibrium. Equal amounts of copper and slag were equilibrated in a molybdenum crucible in order to determine the sulphide capacity. Sulphur was added as Cu<sub>2</sub>S in an amount of 1/10 of that of the slag, and all was dissolved. In each experiment, a certain amount of slag (CMAS), Cu and Cu<sub>2</sub>S was used. The sulphur composition was then measured in both Cu-melt and slag. The sulphur composition in both metal and slag are shown in Fig. 10 for slags with 30 and 35 mass% Al<sub>2</sub>O<sub>3</sub> and 55 mass% CaO. The sulphide capacity is strongly dependent on the composition, and it was found to increase with the basic oxides. The agreement between calculated and experimental data is very good.

## Conclusions

The extended TCOX thermodynamic database, now including sulphur, can be used to make calculations related to steelmaking involving both oxygen and sulphur. It should be emphasised that, although the database covers a large number of elements, not all subsystems are fully assessed. Nevertheless, the equilibrium calculations made by using the database are in good agreement with the reported experimental observations. This includes applications involving oxygen and sulphur separately as well as a combination of the two. The good agreement does not just demonstrate the usability of the thermodynamic database but also the essence of the CALPHAD method, that physically reasonable models and good descriptions of key lower order systems give reliable extrapolations into higher order systems.

**Funding Information** The presented work was performed within the COMPASS project, which was funded by KTH Royal Institute of Technology, Outokumpu Stainless Foundation, Ovako, SSAB EMEA

and Thermo-Calc Software. The project was also associated with the VINN Excellence Center Hero-m, financed by VINNOVA (Grant number 2012–02892), the Swedish Governmental Agency for Innovation Systems, Swedish industry, and KTH Royal Institute of Technology.

**Open Access** This article is distributed under the terms of the Creative Commons Attribution 4.0 International License (<http://creativecommons.org/licenses/by/4.0/>), which permits unrestricted use, distribution, and reproduction in any medium, provided you give appropriate credit to the original author(s) and the source, provide a link to the Creative Commons license, and indicate if changes were made.

## References

- Wang Y, Valdez M, Sridhar S (2002) Formation of CaS on Al<sub>2</sub>O<sub>3</sub>-CaO inclusions during solidification of steels. *Metall Mater Trans B* 33:625–632
- Lange KW (1988) Thermodynamic and kinetic aspects of secondary steelmaking processes. *Int Mater Rev* 33:53–89
- Bigelow LK, Flemings MC (1975) Sulfide inclusions in steel. *Metall Trans B* 6:275–283
- Wranglén G (1974) Pitting and sulphide inclusions in steel. *Corros Sci* 14:331–349
- Kaufman L, Bernstein H (1970) Computer calculation of phase diagrams. Academic Press, New York
- Hillert M, Staffansson L-I (1970) The regular solution model for stoichiometric phases and ionic melts. *Acta Chem Scand* 24:3618–3626
- Hillert M (2001) The compound energy formalism. *J Alloys Compd* 320:161–176
- Hillert M, Kjellqvist L, Mao H, Selleby M, Sundman B (2009) Parameters in the compound energy formalism for ionic systems. *Calphad* 33:227–232
- Hillert M, Jansson B, Sundman B, Ågren J (1985) A two-sublattice model for molten solutions with different tendency for ionization. *Metall Trans A* 16:261–266
- Sundman B (1991) Modification of the two-sublattice model for liquids. *Calphad* 15:109–119
- TCOX7 - TCS Metal Oxide Solutions Database, v7.0 by Thermo-Calc Software AB, 2017
- Seo W, Han W, Kim J, Pak J (2003) Deoxidation equilibria among Mg, Al and O in liquid iron in the presence of MgO Al<sub>2</sub>O<sub>3</sub> spinel. *ISIJ Int* 43:201–208
- Nakasuga T, Nakashima K, Mori K (2004) Recovery rate of chromium from stainless slag by iron melts. *ISIJ Int* 44:665–672
- Douglass DL, Gesmundo F, de Asmundist C (1986) The air oxidation of an austenitic Fe-Mn-Cr stainless steel for fusion-reactor applications. *Oxid Met* 25:235–268
- Dilner D, Mao H, Selleby M (2015) Thermodynamic assessment of the Mn-S and Fe-Mn-S systems. *Calphad* 48:95–105
- Lee B, Sundman B, Il Kim S, Chin K (2007) Thermodynamic Calculations on the Stability of Cu<sub>2</sub>S in Low Carbon Steels *ISIJ Int* 47:163–171
- Dilner D, Kjellqvist L, Selleby M (2016) Thermodynamic assessment of the Fe-Ca-S, Fe-Mg-O and Fe-Mg-S systems. *J Phase Equilibria Diffus* 37:277–292
- Dilner D (2016) Thermodynamic description of the Fe-Mn-Ca-Mg-S system. *Calphad* 53:55–61
- Kjellqvist L (2016) Fe-Cr-Cu-Ni-S. Unpublished assessment
- Kang Y-B (2010) Critical evaluations and thermodynamic optimizations of the Mn-S and the Fe-Mn-S systems. *Calphad* 34:232–244
- Hillert M, Staffansson L-I (1976) A thermodynamic analysis of the phase equilibria in the Fe-Mn-S system. *Metall Trans B* 7:203–211
- Miettinen J, Hallstedt B (1998) Thermodynamic assessment of the Fe-FeS-MnS-Mn system. *CALPHAD* 22:257–273
- Othani B, Oikawa K, Ishida K (2000) High temp. *Mater Process* 19:197–210
- Wriedt HA, Hu H (1976) The solubility product of manganese sulfide in 3 pct silicon-iron at 1270 to 1670 K *Metall Trans A* 7:711–718
- Ryan MP, Williams DE, Chater RJ, Hutton BM, McPhail DS (2002) Why stainless steel corrodes. *Nature* 415:770–774
- Henthorne M (1970) Corrosion of resulfurized free-machining stainless steels. *Corrosion* 26:511–528
- Ono K, Kohno T (1980) Effect of Inclusion Composition on Stability of Inclusions and Corrosion Resistance of 18-8 Stainless Steel *DENKI-SEIKO* 51:122–131
- Dilner D, Selleby M (2017) Thermodynamic description of the Fe-Ca-O-S system. *Calphad* 57:118–125
- Dilner D, Lu Q, Mao H, Xu W, van der Zwaag S, Selleby M (2014) Process-time optimization of vacuum degassing using a genetic alloy design approach. *Materials (Basel)* 7:7997–8011
- O'Neill HSC, Mavrogenes JA (2002) The sulfide capacity and the sulfur content at sulfide saturation of silicate melts at 1400 °C and 1 bar. *J Petrol* 43:1049–1087
- Ban-Ya S, Hobo M, Kaji T, Itoh T, Hino M (2004) Sulphide capacity and sulphur solubility in CaO-Al<sub>2</sub>O<sub>3</sub> and CaO-Al<sub>2</sub>O<sub>3</sub>-CaF<sub>2</sub> Slags. *ISIJ Int* 44:1810–1816
- Allertz C, Sichen D (2015) Sulfide capacity in ladle slag at steel-making temperatures. *Metall Mater Trans B* 46:2609–2615